

AD-A169 715

A STUDY OF SURFACE DAMAGE AT LOW-AMPLITUDE SLIP(U)
NAVAL AIR DEVELOPMENT CENTER WARMINSTER PA AIRCRAFT AND
CREW SYSTEMS TECHNOLOGY DIRECTORATE P KENNEDY JUN 86
NADC-86070-60

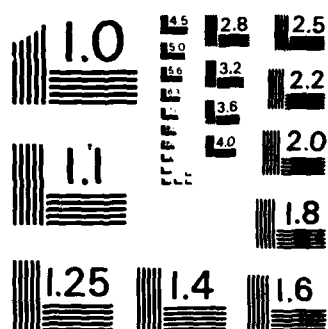
1/1

UNCLASSIFIED

F/G 11/6

NL





MICROCOPY RESOLUTION TEST CHART
NATIONAL BUREAU OF STANDARDS-1963-A



A STUDY OF SURFACE DAMAGE AT LOW-AMPLITUDE SLIP

Paul Kennedy

Aircraft and Crew Systems Technology Directorate
NAVAL AIR DEVELOPMENT CENTER
Warminster, Pennsylvania 18974

FINAL REPORT

AIRTASK NO. A-320-320A/001-B/1F61-542-000
WORK UNIT ZM510

Approved for Public Release: Distribution is Unlimited.

Prepared for
NAVAL AIR SYSTEMS COMMAND
Department of the Navy
Washington, DC 20361

DTIC
ELECTE
JUL 24 1986
S D E

86 20

AD-A169 715

DTIC FILE COPY

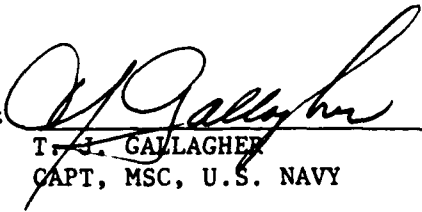
NOTICES

REPORT NUMBERING SYSTEM - The numbering of technical project reports issued by the Naval Air Development Center is arranged for specific identification purposes. Each number consists of the Center acronym, the calendar year in which the number is assigned, the sequence number of the report within the specific calendar year, and the official 2-digit correspondence code of the Command Office or the Functional Directorate responsible for the report. For example: Report No. NADC-78015-20 indicates the fiftieth Center report for the year 1978, and prepared by the Systems Directorate. The numerical codes are as follows:

CODE	OFFICE OR DIRECTORATE
00	Commander, Naval Air Development Center
01	Technical Director, Naval Air Development Center
02	Comptroller
10	Directorate Command Projects
20	Systems Directorate
30	Sensors & Avionics Technology Directorate
40	Communication & Navigation Technology Directorate
50	Software Computer Directorate
60	Aircraft & Crew Systems Technology Directorate
70	Planning Assessment Resources
80	Engineering Support Group.

PRODUCT ENDORSEMENT - The discussion or instructions concerning commercial products herein do not constitute an endorsement by the Government nor do they convey or imply the license or right to use such products.

APPROVED BY:


T. J. GALLAGHER
CAPT, MSC, U.S. NAVY

DATE

22 August 1985

UNCLASSIFIED

SECURITY CLASSIFICATION OF THIS PAGE

A169715

REPORT DOCUMENTATION PAGE

1a REPORT SECURITY CLASSIFICATION Unclassified			1b RESTRICTIVE MARKINGS		
2a SECURITY CLASSIFICATION AUTHORITY			3 DISTRIBUTION AVAILABILITY OF REPORT Approved for public release; Distribution is Unlimited.		
2b DECLASSIFICATION/DOWNGRADING SCHEDULE					
4 PERFORMING ORGANIZATION REPORT NUMBER(S) NADC-86070-60			5 MONITORING ORGANIZATION REPORT NUMBER(S) N/A		
6a NAME OF PERFORMING ORGANIZATION Naval Air Development Center		6b OFFICE SYMBOL (if applicable) 6061	7a NAME OF MONITORING ORGANIZATION N/A		
6c ADDRESS (City, State, and ZIP Code) Warminster, PA 18974			7b ADDRESS (City, State, and ZIP Code) N/A		
8a NAME OF FUNDING SPONSORING ORGANIZATION Naval Air Systems Command		8b OFFICE SYMBOL (if applicable)	9 PROCUREMENT INSTRUMENT IDENTIFICATION NUMBER		
8c ADDRESS (City, State, and ZIP Code) Washington, DC 20361			10 SOURCE OF FUNDING NUMBERS		
			PROGRAM ELEMENT NO	PROJECT NO	TASK A-320- NO 320A/001-B/ 1F61-542-000
					WORK UNIT ACCESSION NO ZM510
11 TITLE (Include Security Classification) A Study of Surface Damage at Low Amplitude Slip					
12 PERSONAL AUTHOR(S) Paul Kennedy					
13a TYPE OF REPORT Final		13b TIME COVERED FROM TO		14 DATE OF REPORT (Year, Month, Day) June 1986	
15 PAGE COUNT					
16 SUPPLEMENTARY NOTATION					
17 COSATI CODES			18 SUBJECT TERMS (Continue on reverse if necessary and identify by block number)		
FIELD	GROUP	SUB-GROUP	Fretting Tests Metal Microslip Wear Friction Carbon Steel		
19 ABSTRACT (Continue on reverse if necessary and identify by block number) <p>The effect of extremely small slip amplitudes (0 to 5 μm) on transitions in the fretting process such as initiation of surface damage, development of severe surface damage, microcrack initiation and the development of mild wear, was investigated. For SAE 52100 against SAE 52100 steel, the minimum slip amplitude associated with the onset of mild oxidation or surface staining was approximately 0.06 μm. Studies at higher amplitudes of motion indicated a transition from minimal surface damage to severe or significant damage at 2.8 μm. A further slight increase in amplitude to approximately 3.0 μm resulted in a transition into a regime characterized by fatigue crack formation. These transformations were found to be influenced to some extent by material composition and hardness. The onset of severe surface damage occurred at 1.1 μm for SAE 52100 against SAE 1018 and at 0.5 μm for a nickel chrome Hastelloy B alloy against SAE 1018 steel. In general, the amplitude of microslip characterizing the transition from extremely mild to severe damage was found to increase with increasing material hardness.</p>					
20 DISTRIBUTION AVAILABILITY OF ABSTRACT <input type="checkbox"/> UNCLASSIFIED UNLIMITED <input checked="" type="checkbox"/> SAME AS RPT <input type="checkbox"/> DTIC USERS			21 ABSTRACT SECURITY CLASSIFICATION Unclassified		
22a NAME OF RESPONSIBLE INDIVIDUAL Paul Kennedy			22b TELEPHONE (Include Area Code)		22c OFFICE SYMBOL 6061

NADC-86070-60

TABLE OF CONTENTS

	Page No.
BACKGROUND	1
EXPERIMENTAL.....	2
APPARATUS AND PROCEDURES	2
WEAR SCAR ANALYSIS.....	3
MATERIALS AND OPERATING PROCEDURES	3
RESULTS AND DISCUSSION	4
SAE 52100/SAE 52100 STEEL COMBINATION.....	4
OTHER MATERIAL COMBINATIONS	6
CONCLUSIONS	6
REFERENCES	7

Accession For	
NTIS GRA&I	<input checked="checked" type="checkbox"/>
DTIC TAB	<input type="checkbox"/>
Unannounced	<input type="checkbox"/>
Justification	
By _____	
Distribution/	
Availability Codes	
Dist	Avail and/or Special
A-1	



LIST OF ILLUSTRATIONS

Figure No.		Page No.
1	Schematic Drawing of Fretting Test Rig Showing the Configuration of the Ball and Flat Test Specimens.	9
2	Schematic Drawing of the Drive Unit for the Fretting Test Rig Illustrating the Motion Generated at the Ball/Flat Interface	10
3	Ball-on-Flat Configuration Showing the Relationship of the Normal and Shear Stress Distributions and Coefficient of Friction in Determining Wear Scar Dimensions	11
4	Wear Scars on SAE 52100 Steel Flat Specimens at X100 Magnification. Wear Scars on the SAE 52100 Ball Specimens were Identical	12
5	Diameter of the Locked Region and the Outer Diameter of the Wear Scar Plotted as a Function of Slip Amplitude for SAE 52100 Versus SAE 52100	13
6	Surface Profiles of Wear Scars for Different Material Combinations at Various Slip Amplitudes	14
7	A Comparison of the Theoretically Predicted Diameter of the Locked Region Based on Elastic Analysis with Experimental Results	15
8	Photomicrographs of Wear Scars Formed with SAE 52100 Steel Specimens Showing Expanded Views of the Slipped Region. Magnifications were X160, X800 for (a) and (b) and X280, X2800 for (c) and (d).	16
9	An Elastic Model That Takes into Account the Possibility of Plastic Deformation of Asperities in the Ball/Flat Contact Area. The Dark and Light Circles Represent the Relative Displacements of the Flat and Ball Surfaces, Respectively.	17
10	Photomicrographs of Wear Scars Showing the Formation of Micro-cracks in the Slipped Region at X160 and X800 Magnification.	18
11	The Effect of Material Hardness on Surface Damage.	19

BACKGROUND

Fretting is a peculiar type of surface damage that results from the small oscillatory motion of two contacting solid surfaces. Fretting damage is characterized by one or more of the following: surface roughening, metal transfer, crack formation with propagation and material removal or wear. Fretting wear is usually characterized by the formation of copious amounts of wear debris. The consequences of fretting can be varied and are dependent on the specific situation or fretting condition. It has been found that fretting can result in either excessive wear, surface fatigue, component fracture, loss of clamping pressure or possibly jamming due to generated debris. In order to reduce fretting, it is necessary to obtain a correlation between the type of surface damage and specific fretting conditions.

Although many parameters such as atmosphere, stress magnitude, frequency, temperature, hardness, finish and contact area have been shown to effect the magnitude of fretting, the most significant variables are the materials and the slip amplitude which can be controlled in the design process. Thus, it would be desirable to obtain a correlation between surface damage and slip amplitude for different material combinations.

The range of motion associated with fretting damage has not been clearly defined. On the lower end of the scale, Tomlinson (1) in 1927 found evidence that relative motion or slip between two surfaces could occur at amplitudes as small as $0.002\text{ }\mu\text{m}$. This value seems small since it is of the order of molecular dimensions. At the other end, it is reasonable to expect that the upper amplitude limit would be marked by the transition from the fretting wear process to wear more characteristic of unidirectional sliding. Halliday (2) and Ohmae and Tsukizoe (3) believe that this upper limit would be $250 - 300\text{ }\mu\text{m}$. Between these two limits, the effect of slip amplitude has been widely investigated. Several investigators (3, 4, 5, 6) have reported the existence of a critical slip amplitude, usually somewhere between 30 and $70\text{ }\mu\text{m}$, at which the fretting wear rate increases significantly. Slip amplitudes significantly below this critical amplitude are generally assumed to be characterized more by surface damage and fatigue rather than wear. Unfortunately, very few studies have been conducted in this low amplitude range even though studies have indicated its importance in roller contact bearings (7), clamped joints (8), pivots (9) and a variety of aircraft components (10).

Bill has conducted a number of studies concerned with fretting fatigue, surface damage and wear with particular emphasis on the role of the surface oxide (11, 12, 13, 14). He has found that wear increases significantly above $25\text{ }\mu\text{m}$ and that wear is not linear with sliding distance but with number of cycles which suggests a fatigue type mechanism rather than adhesion. Below $25\text{ }\mu\text{m}$, the damage mechanism is the same, crack generation and propagation, but this apparently does not result in wear particles. In general, four types of sliding behavior were observed. Type I was characterized by adhesion and plastic flow, Type II involved oxidation and film removal with each cycle, Type III was characterized by fatigue with oxidation accelerating the process and Type IV involved surface slip on an oxide film. Very early in the fretting process, Type I behavior predominates but this is transformed into one of the others depending on the nature of the materials and their oxide films. The fatigue process is similar to that characterizing low cycle fatigue. It is interesting to note that the wear coefficient in the high fretting wear region ($25\text{ }\mu\text{m}$) are of the order of 10^{-7} to 10^{-9} ; this is much lower than that found in unlubricated nonfretting sliding (10^{-3} to 10^{-5}). This is probably due to the ineffectiveness of wear particle formation at low slip amplitudes under fretting conditions.

Most studies have been made using slip amplitudes greater than $10\text{ }\mu\text{m}$. The studies herein are primarily concerned with the low amplitude fretting damage that occurs before the onset of accelerated wear. Investigations were conducted in the 0 to $10\text{ }\mu\text{m}$ range with different material combinations to define the nature of surface damage and how it progresses. Such data could be used to develop design criteria or define appropriate material combinations for the range of application. The results of this investigation form the basis of this report. This work was performed under AIRTASK A-320-320A/001-B/1F61-542-000, Work Unit No. ZM510.

EXPERIMENTAL

APPARATUS AND PROCEDURES

Most conventional test rigs generate fretting wear by imparting a linear oscillatory motion on two contacting specimens under load conditions. This back and forth motion requires a physical displacement of one specimen relative to the other with the displacement equal to the magnitude of slip. Alternately, a similar type of fretting motion would be produced by twisting one specimen relative to the other. In this case, the magnitude of slip would be proportional to the angle of twist. This latter approach was taken in this investigation using a ball and flat specimen. The ball was loaded against the flat to produce a Hertzian contact area which defined the actual damage or wear area. With the ball specimen stationary, an oscillatory rotational or twisting motion was imparted to the flat specimen. This motion was about an axis perpendicular and through the center of the Hertzian contact area. The relative motion of the two specimens in the contact area produced fretting damage.

The fretting test rig used in this investigation had previously been used in a pivot fretting study (9) and in an earlier part of this study (15). A schematic of the test rig and the drive unit that powers the test rig are shown in Figures 1 and 2. The fretting test rig shown in Figure 1 provides for the loading of a 12.7 mm diameter ball against a cylindrical flat specimen approximately 8 mm in diameter by 3 mm in height. Components used to mount the ball specimen to the central shaft and the flat specimen to the gas bearing are not shown for the sake of clarity. Information concerning mounting can be found in a previous report (15). This specimen configuration has the advantage that precision ground balls of a variety of different materials are available from several suppliers and flat specimens can be easily machined from rod stock.

Fretting tests were carried out by first loading the ball specimen by means of the bellow-type load cell shown in Figure 1 against the flat specimen. After this, a twisting motion is transmitted to the flat specimen from the drive system shown in Figure 2. The ball is held stationary and motion is limited to the flat. This produces slip in the ball/flat contact area. Loading of the ball against the flat is achieved by increasing the air pressure in the bellow-type load cell which causes the shaft and ball to press down on the flat, which is also loaded upwards by the pressure on the gas bearing. The net difference in the upward and downward forces determine the load.

Controlled movement of the flat specimen was achieved through the use of two electromagnetic drivers attached to the lever arm of the gas bearing. The drive unit consists of two low internal mass 75 watt audio speakers modified by fastening an aluminum cone and a thin steel push rod assembly onto the surface of the speaker cone. This assembly transmitted the vibratory motion of the speaker cones to the lever arm of the gas bearing. The amplitude, frequency and phase relationship of the two drive units were controlled with an oscillator and amplifier in the electrical circuit that powered the drivers.

Capacitance probes were used to measure the frequency and the amount of displacement at the point of attachment of the push rod to the lever arm. This is illustrated in Figure 2. The push rod amplitudes measured by the capacitance probes ranged from 0 to 0.25 mm for these drive units. Since the length of the lever arm from the point of attachment of the push rod to the center of the ball/flat contact area is 8 mm and the radius of the contact area (i.e., the small circle in the center of the flat shown in Figure 2) is 0.15 mm, it is possible to study amplitudes from 0 to 5 μm .

WEAR SCAR ANALYSIS

An analysis of a typical wear scar is presented in Figure 3. This analysis considers a ball resting on a rigid flat plate. Subjecting the ball to a normal load will result in a ball/flat contact area that would be described by the Hertz equations (16). In this Figure, a tangential or shear force, resulting from the action of the drive units, is superimposed on the normal force. The action of these two opposing forces produces relative motion or sliding in the Hertzian contact area.

In order to have relative motion or sliding, a necessary condition is that the applied force must exceed the product of the normal load and the static coefficient of friction, f_s . This criteria can not be applied directly to the ball/flat configuration in Figure 3 because of the complex stress distributions that develop in the contact area. For example, in the case of normal stress (T_N) distribution, the pressure is zero at the edge of the contact area and a maximum at the center, and in the case of the shear stress (T_S) distribution, the pressure will be at maximum at the edge and zero at the center. Estimates regarding the shape of these distributions are presented in Figure 3. The sliding criteria used in this analysis can be stated as:

$$T_S > f_s T_N \quad (1)$$

If f_s is assumed to be unity, reference to Figure 3 indicates that slip will occur only in those areas where T_S exceeds T_N . All other regions not satisfying this requirement will be locked. A typical resulting wear scar is shown on the bottom of Figure 3.

MATERIALS AND OPERATING PROCEDURES

The effect of material and hardness on fretting was investigated using ball/flat combinations that include SAE 52100 (Rc 64) steel against SAE 1018 (Rb 96) steel, a nickel chrome Hastelloy B (Rb 84) alloy against SAE 1018 (Rb 96) and a SAE 52100 (Rc 64) against SAE 52100 (Rc 64). Ball specimens were standard 12.7 mm balls made from either SAE 52100 steel or Hastelloy B. Flat specimens were machined from either SAE 1018 rod stock or SAE 52100, in the annealed state, to required specifications that included surface grinding to a 0.2 μm finish. The SAE 52100 specimens were heat treated to a final hardness of approximately Rc 64. Prior to testing, the flat specimens were hand polished using 0.3 and 0.05 μm alumina, washed in boiling stoddard solvent and rinsed in petroleum ether.

After cleaning, the test specimens were placed in the fretting test rig. The air pressure lines attached to the rig were adjusted to produce a normal load of 88 N. This produced a contact area of about 0.07 mm^2 . Motion was then transmitted to the flat through the drive units. These units were operated at 210 Hz at various input amplitudes. The duration of the test was normally 3 hours. The push rod amplitudes were converted to slip amplitudes occurring at the edge of the ball/flat contact area to simplify the reporting of data.

At the end of the test, specimens were removed and examined microscopically. The nature of the surface damage was recorded in both the locked and slipped regions. The outer diameters of the locked and slipped regions were measured and compared with theoretical values. A more detailed surface analysis was conducted with most specimens. This included SEM, electron diffraction and x-ray analysis. Surface profiles of the wear scar were made to indicate plastic deformation, surface damage and wear. In some cases, the surface were etched with picric acid to yield cracks and subsurface distortions.

RESULTS AND DISCUSSION

SAE 52100/SAE 52100 STEEL COMBINATION

Photomicrographs of wear scars formed by SAE 52100 steel on SAE 52100 steel are shown in Figure 4. These wear scars, formed on the flat specimens, were taken at a magnification of 100 times since they are small and have diameters of approximately 0.3 mm. Wear scars formed on the ball specimens were identical. These photomicrographs show the effect of slip amplitude on wear scar formation. The slip amplitudes in Figure 4 were calculated from the measured push rod amplitudes and represent the amount of microslip at the outer diameter or the Hertz radius.

The primary question concerns the minimum amount of microslip necessary to produce the first indication of damage. Figure 4 indicates that the wear scar formed at a slip amplitude of $0.1 \mu\text{m}$ is not much more than a faint outline of the ball/flat contact area. The measured radius of 0.150 mm compares very favorable with the predicted value of 0.152 mm. Additional tests at slip amplitudes of $0.03 \mu\text{m}$ and below gave no indication of any wear scar. On the basis of these experiments an estimate of $0.06 \mu\text{m}$ would seem reasonable for the minimum amount of microslip necessary to produce the first indication of fretting.

Figure 4 indicates that relatively small increases in slip amplitude produce significant changes in both the amount of surface damage and wear scar dimensions. Wear scar dimensions, which include the outer diameters of the locked and slipped region are presented for these and other wear scars as a function of slip amplitude in Figure 5. In addition, the outer diameter of a second ring that develops at higher slip amplitudes is also included in this figure. This secondary ring can be clearly seen in Photograph (e) in Figure 4. Theory indicates that the outer diameter of the slipped region for all of the wear scars should be equal to the Hertz radius. Since the Hertz radius is a simple function of ball diameter, elastic modules and load, this radius should be independent of slip amplitude. Figure 5 indicates that the outer diameter of the slipped region is independent of slip amplitude for microslip less than $2 \mu\text{m}$. The increase in the diameter of the wear scars at slip greater than $2 \mu\text{m}$ may be due to effects associated with the initiation of surface damage. This estimate of $2 \mu\text{m}$ for the initiation of surface damage was confirmed by surface profile measurements made across the wear scars. The data for SAE 52100/SAE 52100 shown in Figure 6 indicates that the first surface ridges appear at $2.75 \mu\text{m}$ and become increasingly severe at higher slip amplitude.

Elastic theory, as developed in Figure 3, indicates that the diameter of the locked region should decrease with increasing slip amplitude. In order to determine if the slope of the line defining the change in the outer diameter of the locked region in Figure 5 actually corresponds to what would be expected on the basis of elastic theory, a quantitative model capable of predicting the diameter of the locked region as a function of slip amplitude or push rod amplitude would be needed. This requirement was satisfied by a model developed by Deresiewicz (17) for two contacting elastic spheres acted upon by a small oscillating torsional couple. This model is an

extension of theory developed by Mindlin (18). In this analysis, the ratio of the radius of the locked region to the Hertz or load radius, c/a , is expressed as a function of push rod amplitude, or more specifically, the angle of twist, β . The relationship of these parameters are shown in the following equations:

$$c/a = \sqrt{2K^2 + 1} \quad (2)$$

$$\frac{\mu a^2 \beta}{f N} = \frac{3}{16} K^2 \left(1 + \frac{3}{8} K^2 + \frac{15}{64} K^4 + \dots \right) \quad (3)$$

where

- c = Radius of the locked region
- a = Radius of Hertz or load radius
- μ = Shear modulus
- β = Angle of Twist
- f = Coefficient of friction
- N = Applied load

Reference to Figure 2 indicates the relationship of the angle of twist to the push rod amplitude or the slip amplitude calculated at the Hertz radius. This model was used to predict the radius of the locked region using a Hertz radius of 0.152 mm, a shear modulus of 207 GPa and a load of 88 N. A comparison of theoretical data with experimental data is shown in Figure 7. In this plot, a coefficient of friction of 1.5 was used to fit theory with experiment. Although this value seems to be higher than would be predicted, it should be pointed out that this is a static friction condition at high pressures where relative slip had not previously taken place. The important observation is that the trends are similar indicating that the decrease in locked region diameter is probably a function of the increased slip amplitude rather than wear. If a lower coefficient of friction is used, then the decrease in the diameter of the locked region with slip would be more rapid.

The observed formation of a second ring or inner ring can not be explained using elastic theory. One possible explanation is that this inner ring is the result of surface working caused by plastic deformation of asperities rather than damage resulting from slip. The expanded photomicrograph in Figure 8(d), showing the morphology of the inner ring after picric acid etching, tends to suggest a worked surface. This possibility is illustrated in Figure 9. This figure schematically shows the relative position of two points (light and dark circles) located slightly below the surfaces of two contacting asperities. When subjected to increasing amounts of displacement, these two points undergo elastic deformation in the locked region from $r = 0$ to $r = r_e$, both elastic and plastic deformation from $r = r_e$ to $r = c$ and finally elastic and plastic deformation and microslip from $r = c$ to $r = a$. This figure also illustrates the effect of load. If the ball was under zero load, the slip amplitude at any point along the radius of the wear scar would be equal to the height of the slanted dashed line or directly proportional to the push rod amplitude. Under actual load conditions, the expected relative displacement of the ball with respect to the flat would be taken up to a large extent by elastic and possibly plastic deformation. This would result in slip amplitudes being less than would be calculated based on simple geometry except at the Hertz radius since the load is zero and no elastic or plastic deformation can occur.

It is also possible that this second ring exists at lower slip amplitudes but it can not be detected since damage does not result. Thus, the high friction coefficient is needed in the calculations because of the inability to measure the diameter of the true locked region. At this point, however, this concept is purely speculation.

One of the most interesting results found with the SAE 52100 steel combination can be seen in Figure 10. The striations on the ball specimens suggest the formation of fatigue cracks oriented perpendicular to the direction of motion. This damage pattern is identical to that predicted (19) for interactingasperities. In 3 hours, 2.0×10^6 stress cycles would result at a load of 1.7 GPA, thus fatigue is possible. It is generally felt that fatigue predominates in this low slip region. This result tends to confirm this hypothesis although further work is necessary.

OTHER MATERIAL COMBINATIONS

In addition to tests run on SAE 52100 steel, a series of tests were also run with two other material combinations that included a SAE 52100 (Rc 64) ball versus a SAE 1018 (Rb 98) flat and a nickel chrome Hastelloy B ball (Rb 84) versus a SAE 1018 (Rb 98) flat. Preliminary results for these latter material combinations have been reported elsewhere (15). These data can now be compared with the SAE 52100 (Rc 64) versus SAE 52100 (Rc 64) combination.

Surface profile traces across the wear scars are shown in Figure 9 for these three material combinations. For the nickel chrome alloy/SAE 1018 combination, the first evidence of surface damage occurred at $0.53 \mu\text{m}$. For the SAE 52100/SAE 1018 combination, damage occurred at $1.1 \mu\text{m}$. Slip amplitudes of these magnitudes did not produce any measurable surface damage for the SAE 52100/SAE 52100 combination. For this latter combination, surface damage was not noted at slip amplitudes less than $2.75 \mu\text{m}$.

A better estimate of the trend in surface damage with respect to slip amplitude was obtained by plotting average damage volume as a function of slip amplitude. These data are shown in Figure 11. These values were obtained from the surface profile traces of Figure 6 by first determining the average cross-sectional area and then multiplying this value by the length of the average circumference of the slipped region. These data illustrate the effect of material type and hardness on the ability of these materials to resist severe surface damage. On the basis of these plots, it can be seen that the previous estimates of 0.5, 1.1 and $2.8 \mu\text{m}$ are fairly accurate estimates of the minimum amount of microslip necessary to produce the first indications of significant damage. These curves show an exponential relationship between damage volume and slip amplitude except for the SAE 52100/SAE 1018 combination. In this latter case, the surface profiles in Figure 6 indicates a certain amount of metal deformation which would tend to reduce the damage rate. Another interesting aspect of these plots is the rapid fall off of damage volume with increasing slip amplitude for the SAE 52100/SAE 52100 combination. This is probably due to a transition from a surface damage regime to a wear regime at about $3.0 \mu\text{m}$.

CONCLUSIONS

An investigation was carried out to determine the nature of the fretting damage which occurs at small slip amplitudes. Under the conditions of the experiments reported herein, the following conclusions were drawn:

1. A certain amount of motion or slip can occur without producing any indication of surface damage. This safe range of slip amplitudes was from 0 to $0.6 \mu\text{m}$ for SAE 52100 versus SAE 52100 and from 0 to $0.08 \mu\text{m}$ for SAE 52100 versus SAE 1018 steel.
2. Severe surface damage was found at a slip amplitude of $0.5 \mu\text{m}$ for the nickel chrome Hastelloy B alloy versus SAE 1018 steel, $1.1 \mu\text{m}$ for SAE 52100 versus SAE 1018, and $2.8 \mu\text{m}$ for SAE 52100 versus SAE 52100 steel.

3. Mild wear was observed in the case of SAE 52100 versus SAE 52100 steel at approximately the same slip amplitude as surface damage occurred.
4. Surface damage was similar to that generally referred to as galling, however, evidence of fatigue cracking in the slipped region was also noted.

In summary, this investigation has shown a relationship between the input slip amplitude and the nature of surface damage. It was found that very small slip can occur without producing any kind of surface deformation. Slightly greater amounts of slip were found to produce only mild oxidation or staining without producing any noticeable change in surface morphology. For higher slip amplitudes, some mild surface damage developed, but this rapidly changed into a severe damage regime with a small increase in slip amplitude. For still higher slip amplitudes, two phenomena consisting of the development of surface cracks suggestive of fatigue and material loss or wear, appear to occur concurrently. This study supports the findings of Elliot et. al. (7) that fretting can occur at very small slip amplitudes and it also suggests that it should be possible to control damage and wear in the design process by judicious selection of slip amplitudes and material types.

REFERENCES

- (1) Tomlinson, G.A., "The Rusting of Steel Surfaces in Contact," Proceedings of the Royal Society (London), Vol. 115A, 1927, pp. 472-483
- (2) Halliday, J.S. and Hirst, W., "The Fretting Corrosion of Mild Steel," Proceedings of the Royal Society (London), Vol. 236A, 1956, pp. 411-425
- (3) Ohmae, N. and Tsukizoe, T., "The Effect of Slip Amplitude on Fretting," Wear, Vol. 27, 1974, pp. 281-294
- (4) Waterhouse, R.B., "Fretting Corrosion," Pergamon Press, New York, 1972
- (5) Waterhouse, R.B., "Fretting Wear," Proceedings of the 1981 International Conference, San Francisco, California, American Society of Mechanical Engineers, April 1981, pp. 17-22
- (6) Bill, R.C., "Review of Factors that Influence Fretting Wear," Materials Evaluations under Fretting Conditions, ASTM STP 780, American Society for Testing and Materials, 1982, pp. 165-182
- (7) Elliot, K.B., Mabie, H.H., Furey, M.J., and Mitchell, L.D., "A Vibration Analysis of a Bearing Cartridge Interface for a Fretting Corrosion Study," Paper E-13 presented at the ASLE/ASME Joint Lubrication Conference, Washington, DC, October 1982
- (8) Waterhouse, R.B., "Physics and Metallurgy of Fretting", AGARD Conference Proceedings No. 161, National Technical Information Service, Springfield, Virginia 1974
- (9) Peterson, M.B., Geren, B.F., Arnas, E.B., Gray, S., Murray, S.F., Lund, J.W., and Ling, F.T., "Analytical and Experimental Investigation of Gas Bearing Tilting Pad Pivots," Mechanical Technology Incorporated, NASA CR 72609 (MTI TR-32), 1969

NADC-86070-60

- (10) Hoeppner, D.W., "Fretting of Aircraft Control Surfaces," AGARD Conference Proceedings No. 161, National Technical Information Service, Springfield, Virginia, 1974
- (11) Bill, R.C., "Study on Fretting Wear in Titanium, Monel-400 and Cobalt-25 Percent Molybdenum", American Society of Lubrication Engineers Transactions, Vol. 16, No. 4, 1973, p. 286
- (12) Bill, R.C., "Fretting of AISI 9310 Steel and Selected Fretting-Resistant Surface Treatments," American Society of Lubrication Engineers Transactions, Vol. 21, No. 3, 1978, p. 236
- (13) Bill, R.C., "Fretting Wear of Iron, Nickel and Titanium Under Varied Environmental Conditions," AVRADCOM Research and Technology Laboratories, NASA Lewis Research Center, Cleveland, Ohio
- (14) Bill, R.C., "The Role of Oxidation in the Fretting Wear Process," AVRADCOM Research and Technologies Laboratory, NASA-Lewis Research Center, Cleveland, Ohio
- (15) Kennedy, P.J., Peterson, M.B., and Stallings, L., "An Evaluation of Fretting at Small Slip Amplitudes," Materials Evaluation under Fretting Conditions, ASTM STP 780, American Society for Testing and Materials, 1982, pp. 30-48
- (16) Winer, W.O., and Cheng, H.S., "Film Thickness, Contact Stress and Surface Temperature," The Wear Control Handbook, ASME, New York, 1980, pp. 81-142
- (17) Deresiewicz, H., "Contact of Elastic Spheres Under an Oscillating Torsional Couple," Journal of Applied Mechanics, Trans. ASME, Vol. 76, 1954, pp. 52-56
- (18) Mindlin, R.D., "Compliance of Elastic Bodies in Contact," Journal of Applied Mechanics, Trans. ASME, Vol. 71, 1949, pp. 259-268
- (19) Collins, J.A., Failure of Materials in Mechanical Design, John Wiley and Sons, New York, 1981, pp 482

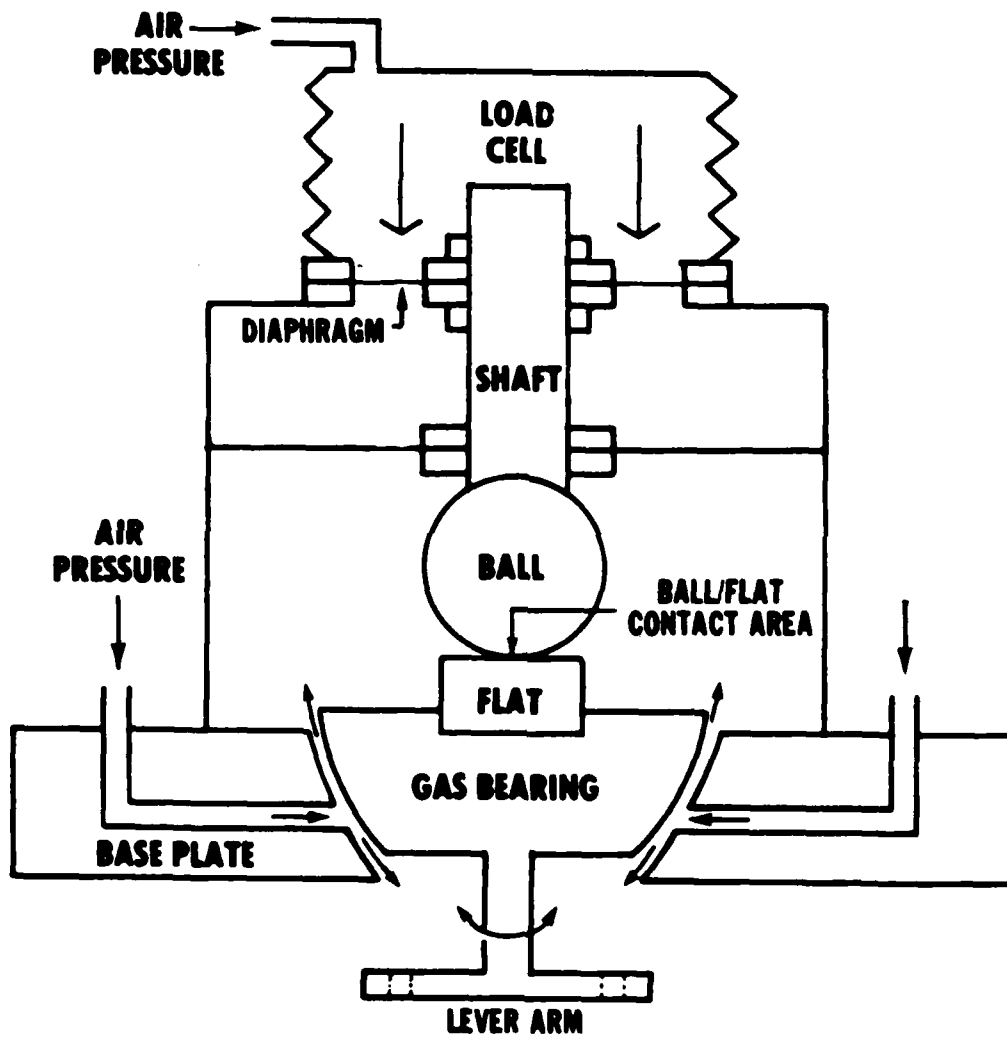


Figure 1. Schematic drawing of fretting test rig showing the configuration of the ball-and-flat test specimens.

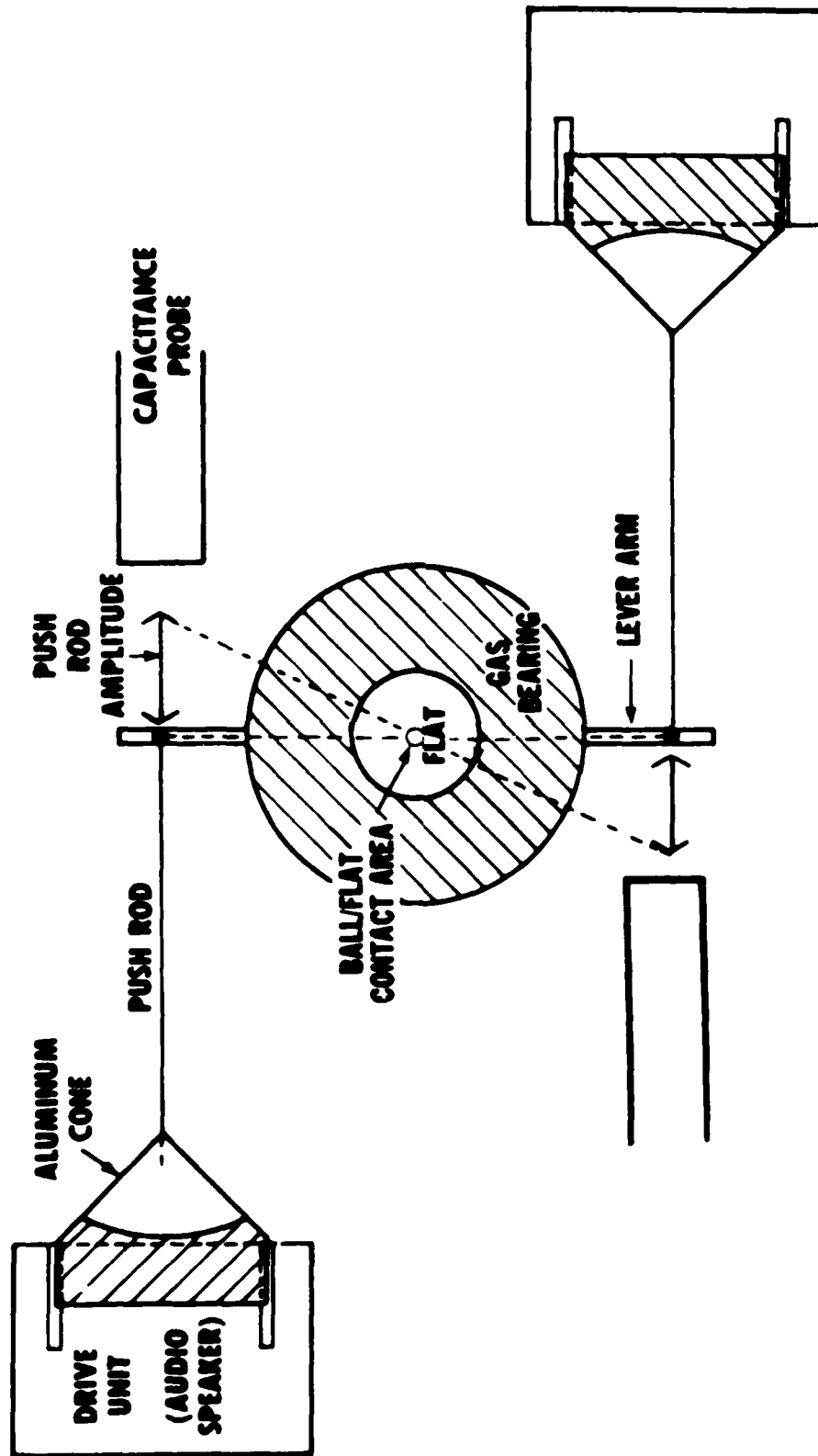


Figure 2. Schematic drawing of the drive unit for the fretting test rig illustrating the motion generated at the ball/flat interface.

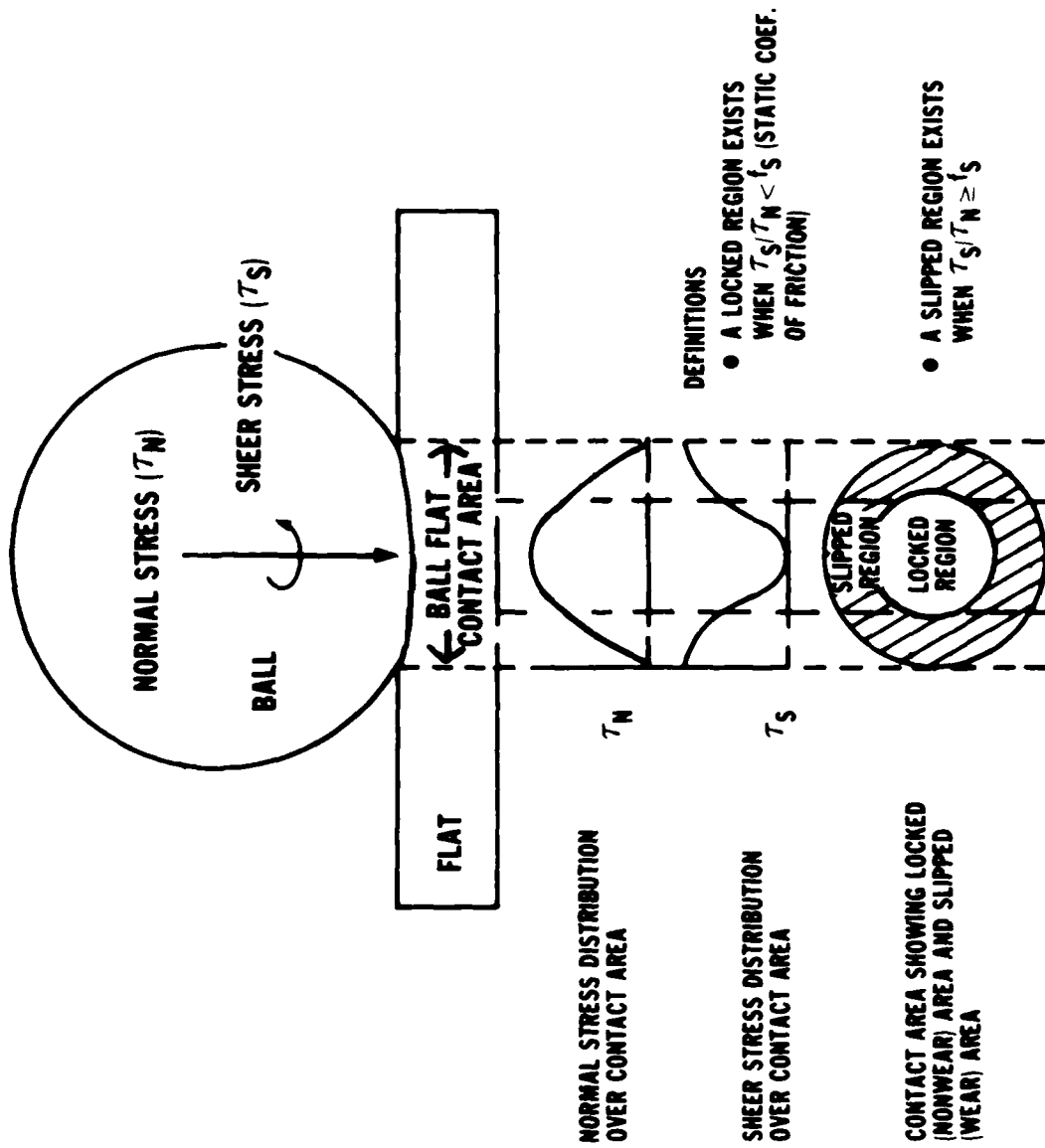


Figure 3. Ball-on-flat configuration showing the relationship of the normal and shear stress distributions and coefficient of friction in determining wear scar dimensions.

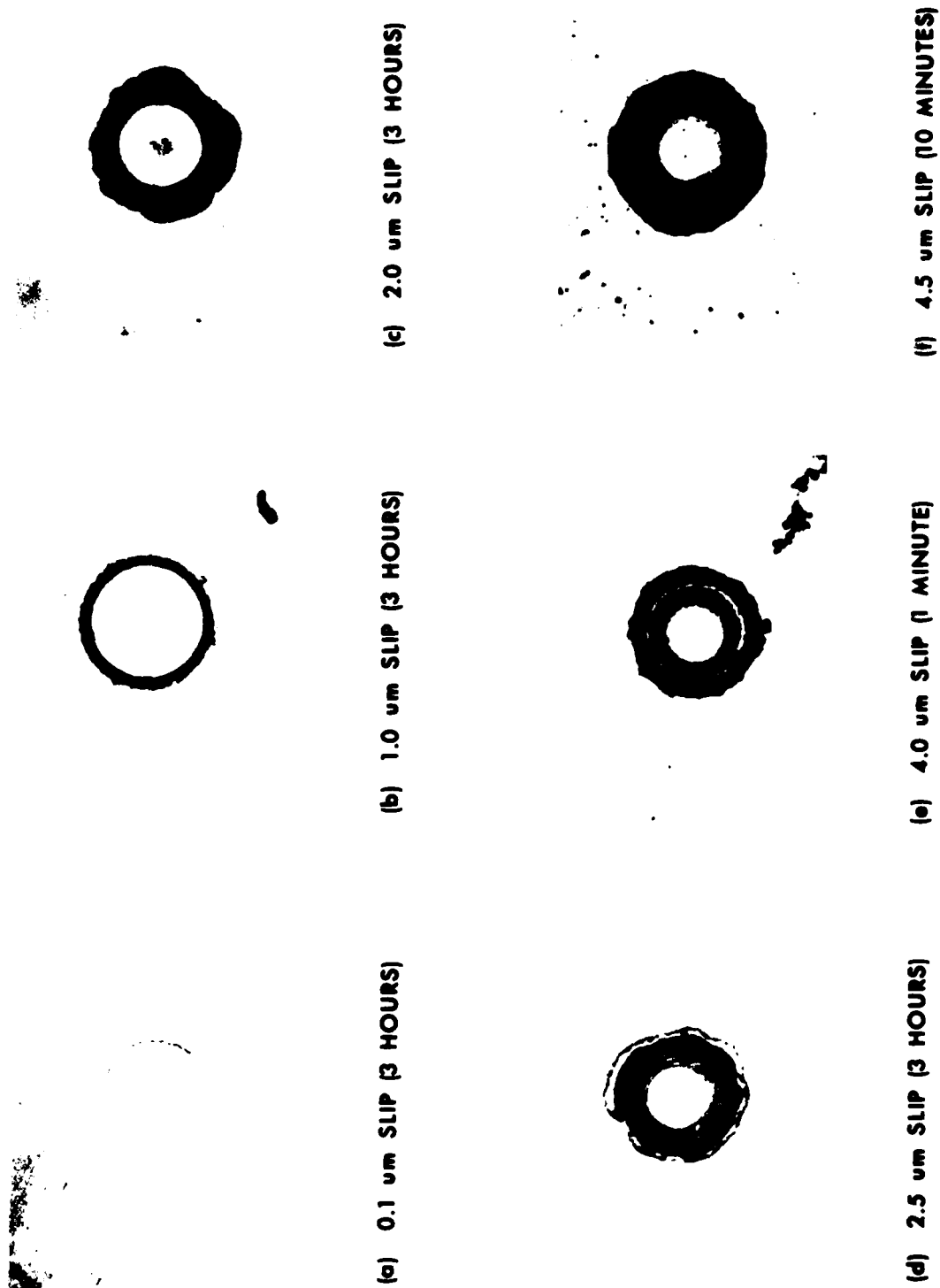


Figure 4. Water scars on SAE 52100 steel flat specimens at X100 magnification. Wear scars on the SAE 52100 ball specimens were identical.

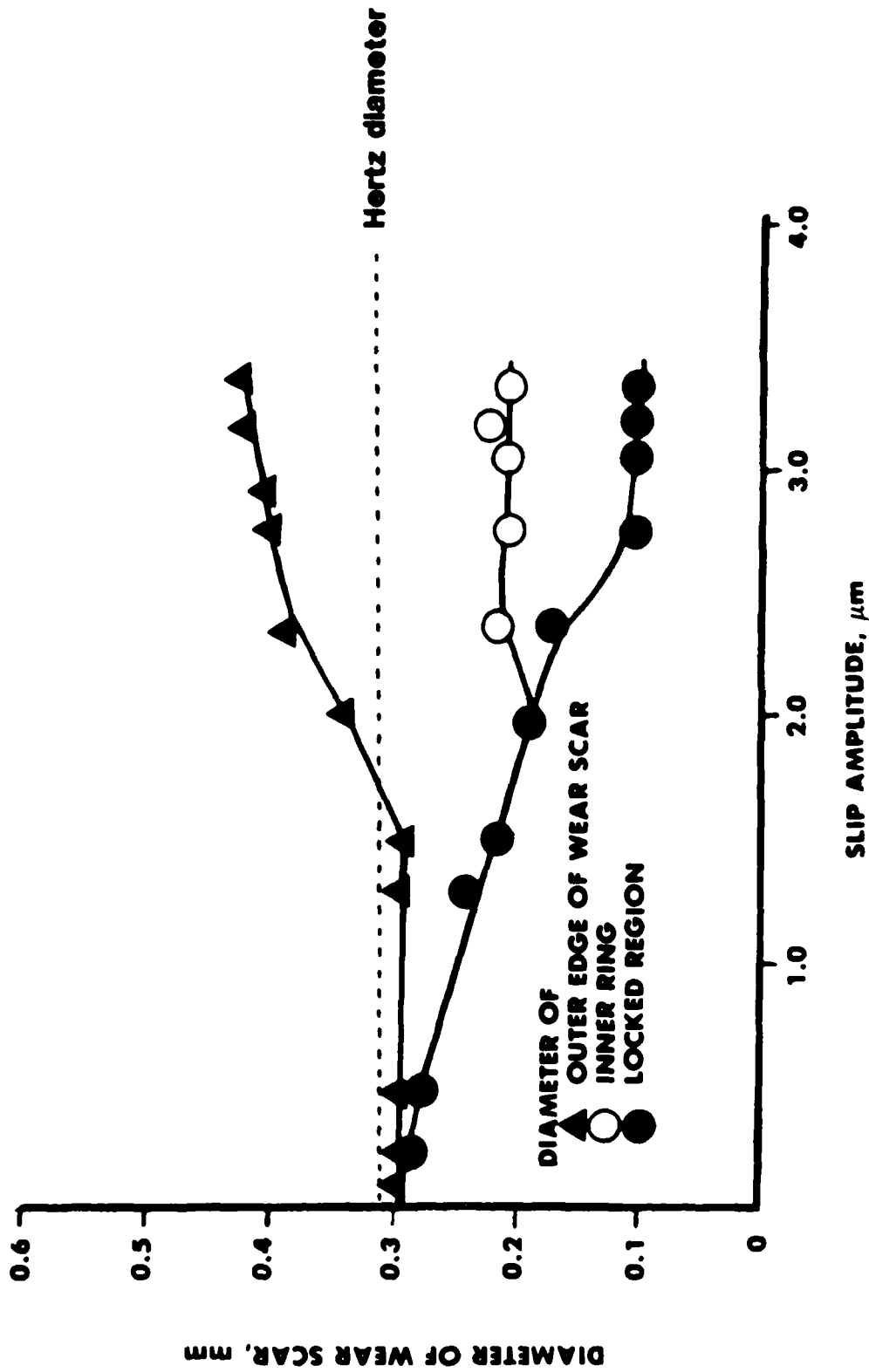


Figure 5. Diameter of the locked region and the outer diameter of the wear scar plotted as a function of slip amplitude for SAE 52100 versus SAE 52100.

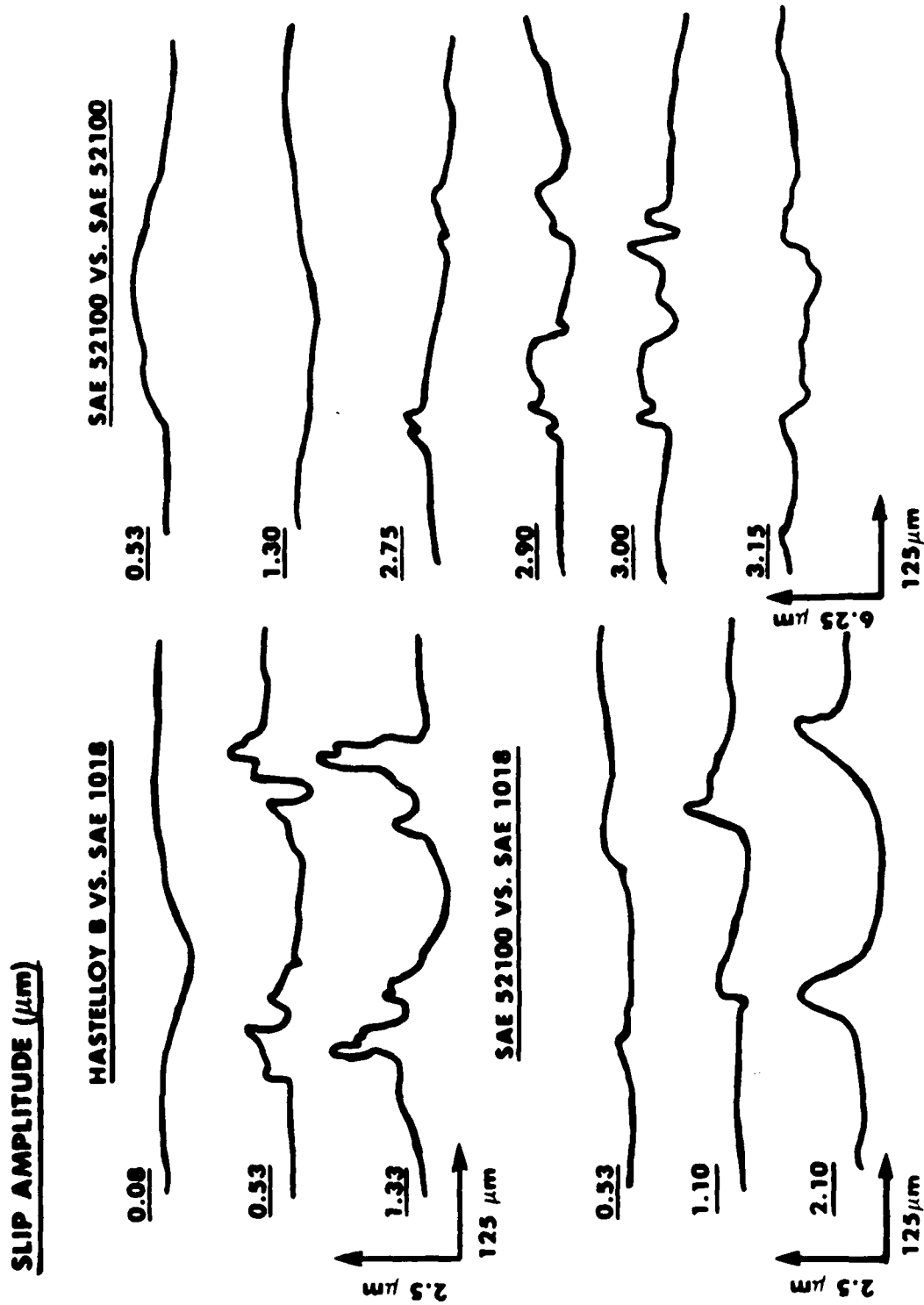


Figure 6. Surface profiles of wear scars for different material combinations at various slip amplitudes.

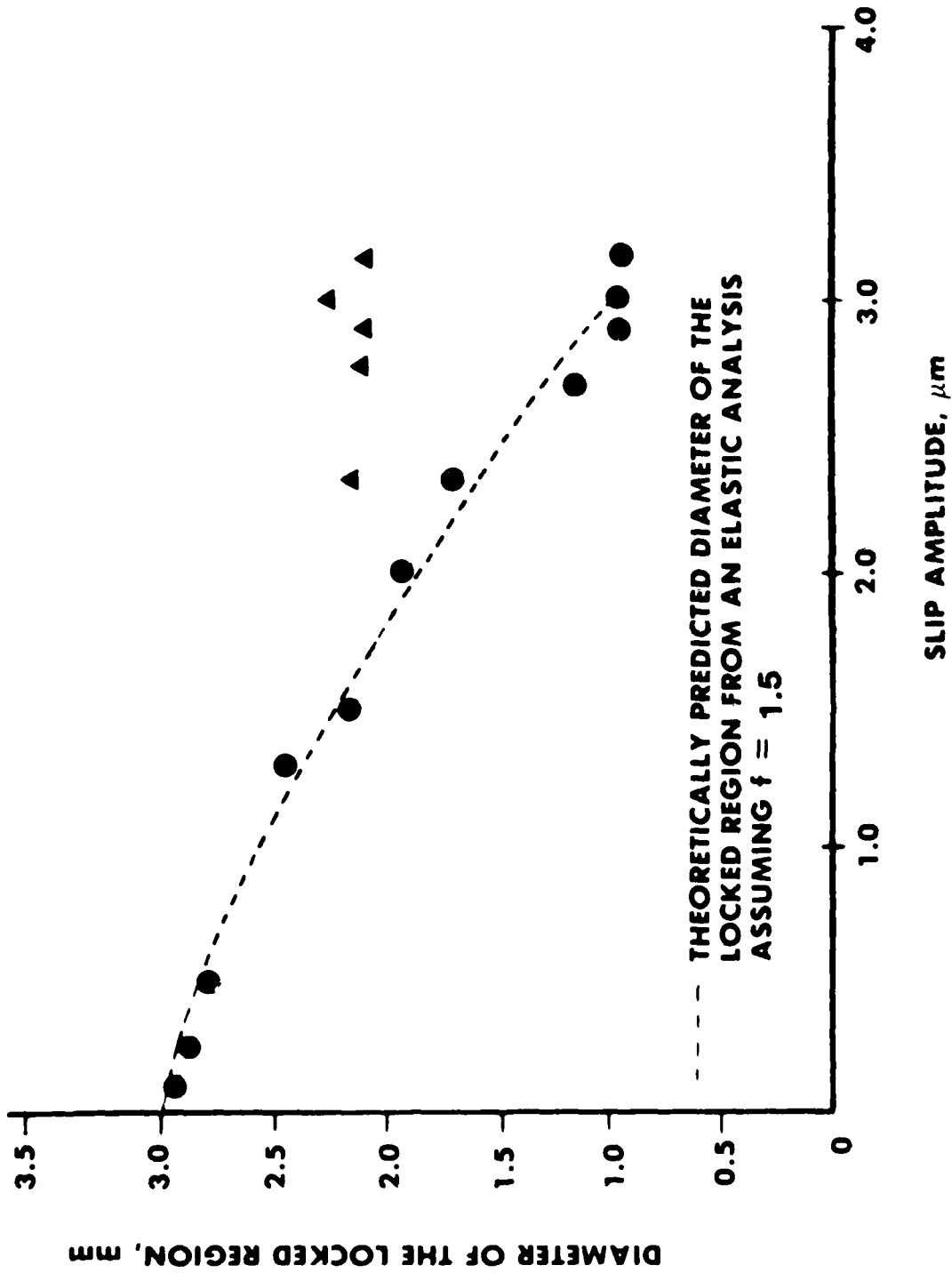


Figure 7. A comparison of the theoretically predicted diameter of the locked region based on elastic analysis with experimental results.

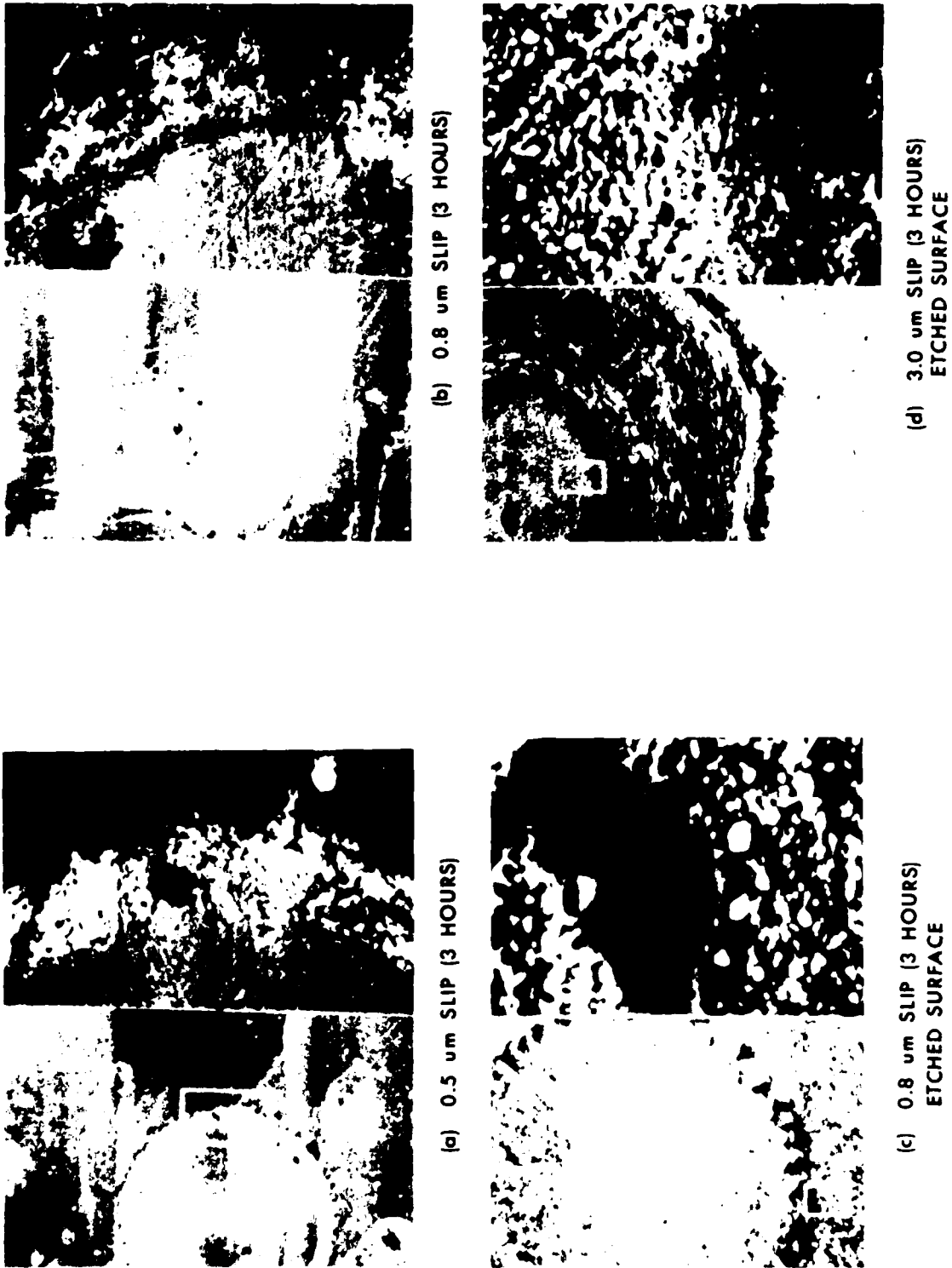


Figure 8. Photomicrographs of wear scars formed with SAE 52100 steel specimens showing expanded views of the slipped region. Magnifications were X160, X280 for (a) and (b) and X280, X2800 for (c) and (d).

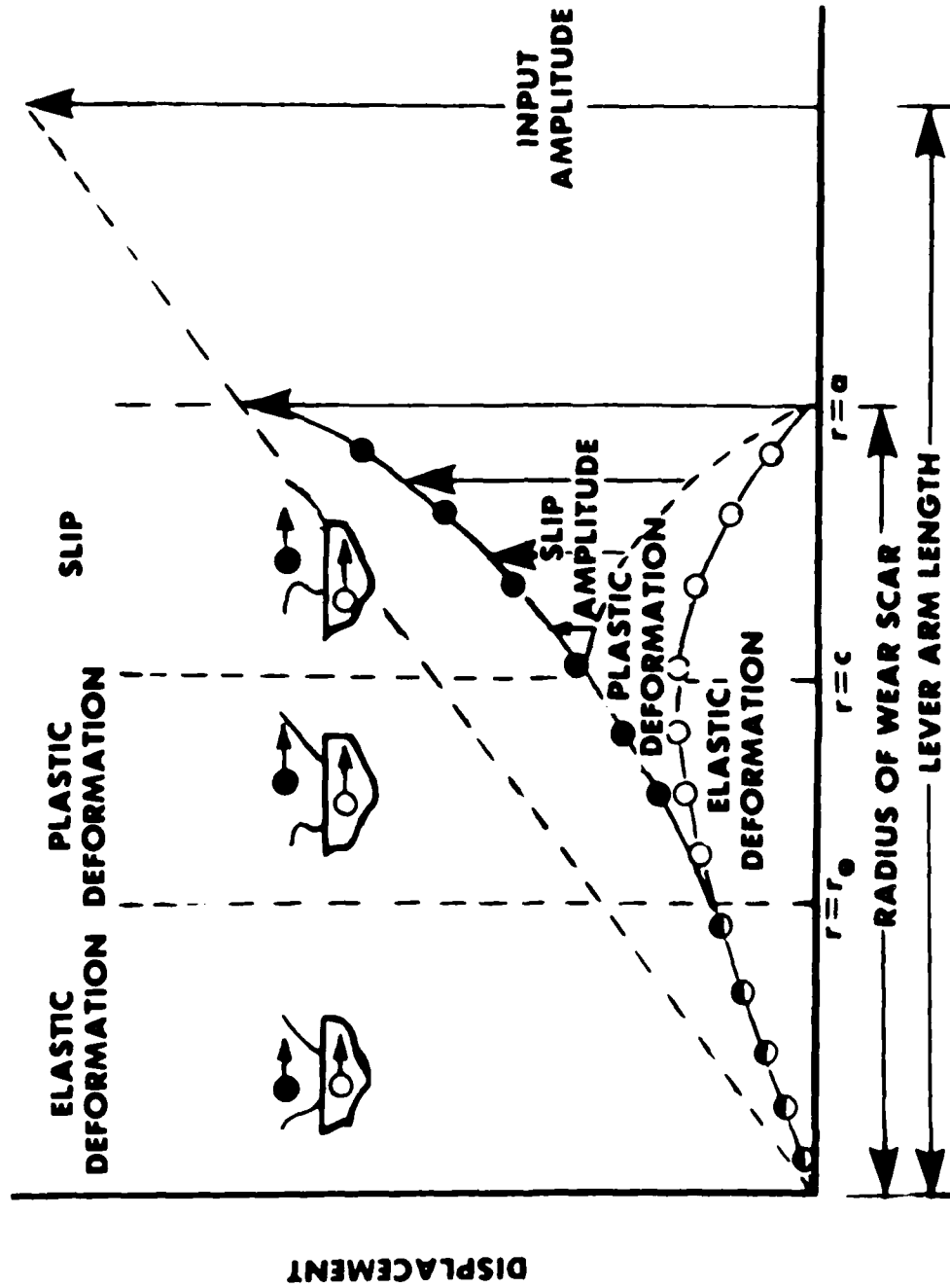
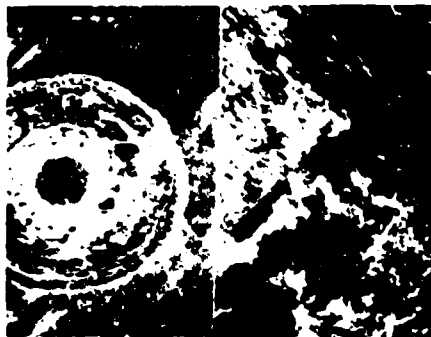
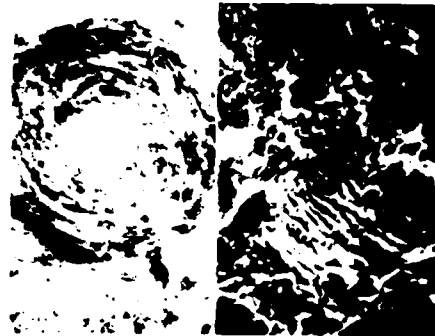


Figure 9. An elastic model that takes into account the possibility of plastic deformation of asperities in the ball/flat contact area. The dark and light circles represent the relative displacements of the flat-and-ball surfaces, respectively.

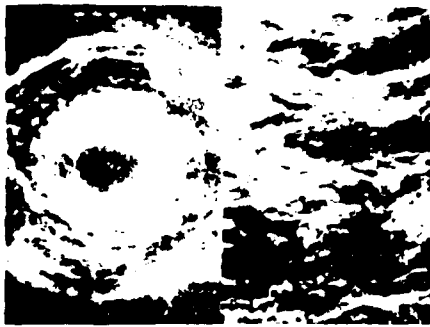


FLAT

(a) 2.9 μm SLIP (3 HOURS)

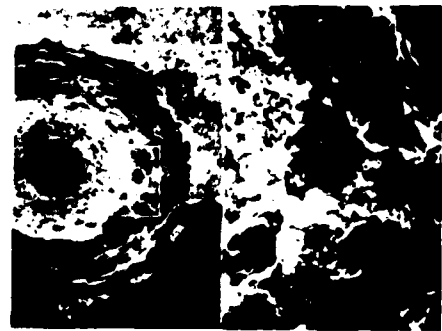


BALL

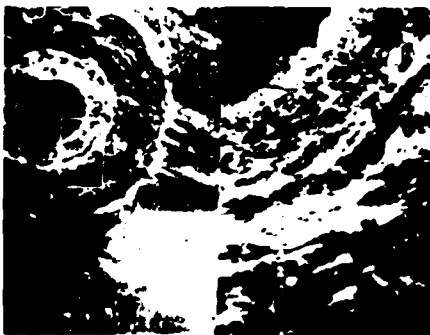


FLAT

(b) 3.0 μm SLIP (3 HOURS)

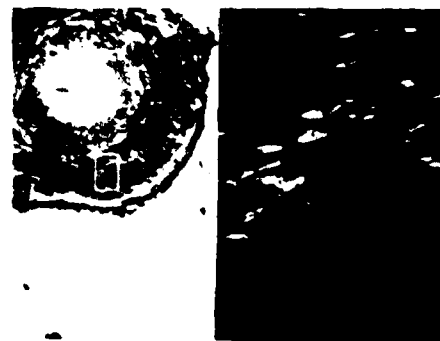


BALL



FLAT

(c) 3.15 μm SLIP (3 HOURS)



BALL

Figure 10. Photomicrographs of wear scars showing the formation of microcracks in the slipped region at X160 and X800 magnification.

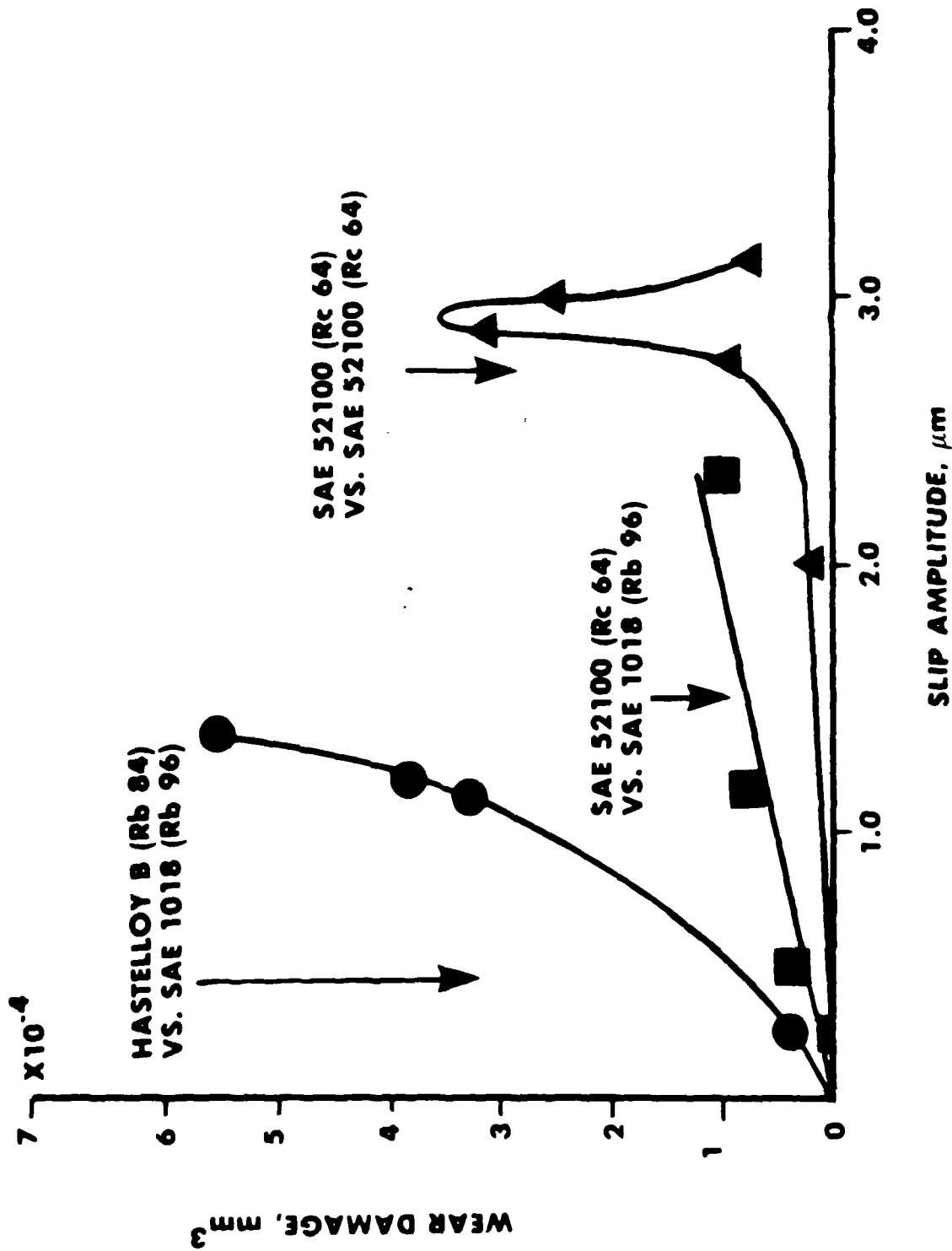


Figure 11. The effect of material hardness on surface damage.

END

DTIC

8-86